C1.4 Vortex Transport by Uniform Flow

1. Code description

XFlow is a high-order discontinuous finite element library written in ANSI C, intended to be run on Linux-type platforms. XFlow supports DG and HDG discretizations and a variety of equation sets, including compressible Euler, Navier-Stokes, and RANS with the Spalart-Allmaras model. High-order is achieved compactly within elements using various high-order bases on triangles, tetrahedra, quadrilaterals, and hexahedra. Parallel runs are supported using domain partitioning and MPI communication. Visual post-processing is performed with an in-house plotter. Output-based adaptivity is available using discrete adjoints.

2. Case summary

The prescribed initial condition was imposed via least-squares projection onto the space spanned by the DG basis at each order. Time stepping was performed using a fifth-order explicit Runge-Kutta scheme.

At each stage of the time stepping scheme, the residual was converged to an absolute L_1 norm below 10^{-12} using a conservative state vector. The freestream quantities provided in the problem description are in SI units, but we found that setting up the problem in these units made the desired iterative convergence of the momentum equations difficult to achieve. This is because the code monitors L_1 norm of the entire state vector for convergence. Also, due to the large values of energy and limits of machine precision, driving this norm below $\sim 5 \times 10^{-7}$ was not feasible for all meshes. Therefore, the input conditions were normalized using $R_{gas} = 1, p_\infty = 1, T_\infty = 1$. This means that nondimensional velocities are related to the physical velocities via the factor $\sqrt{(287.15J/(kg \cdot K)) \cdot (300K)}$, and hence this factor was used to multiply the computed L_2 errors for consistency.

The runs were performed in serial on the *flux* high performance computing cluster at the University of Michigan. On one core of this machine, one TauBench unit is equivalent to 6.61 seconds of compute time.

3. Meshes

Triangular meshes were constructed using an in-house Matlab script. This script created a uniform lattice over the square domain and then created right triangles by bisecting each square along one of the diagonals. Random perturbations to the mesh (for the requested case) were added according to the specified maximum displacement $\delta_{max} = 0.15h$. We note that the perturbed mesh sequence is not nested in that the perturbations were imposed independently on each mesh in the sequence. Sample meshes are shown in Figure 1

4. Results

The figures and tables below present the requested results. RK5 was used for the temporal discretization. The number of time steps for the coarsest mesh (8×8) in each run was set as listed in Table 1. Each number was doubled for every successively-refined mesh in order to maintain the same CFL number. According to sensitivity studies of the time step size, the choices made in Table 1 are close to the optimal values for computation efficiency.

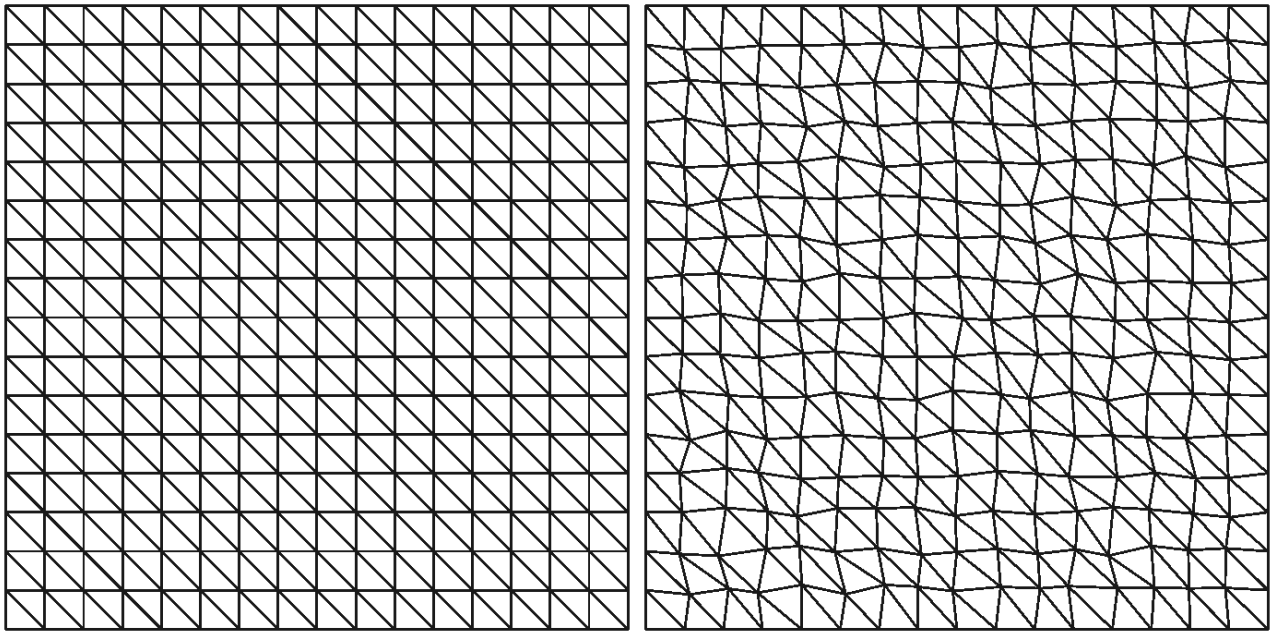

Unperturbed mesh Perturbed mesh

Figure 1: Sample unperturbed and perturbed meshes generated for this case

Case	p = 1	p = 2	p = 3	p = 4
Fast vortex	3150	5200	8000	11500
Slow vortex	25000	42000	65000	90000

Table 1: The number of time steps used for each run on the coarsest mesh with 128 triangular elements

Slow vortex: $M_\infty = .05, \beta = .02, R = .005$

Figure 2 shows the convergence of a conservative state vector L_2 error with mesh refinement. Note that the ideal convergence is indicated by dash-dot lines with the corresponding rate labeled. Table 2 and Table 3 tabulate the L_2 error with convergence rate. Figure 4 and Figure 3 draw a comparison of errors and convergence rates between different numbers of revolutions of the vortex transport. Note that the convergence rates for 1-revolution results are labeled. Figure 5 shows the same error versus work units.

Fast vortex: $M_\infty = .5, \beta = .2, R = .005$

Figure 6 shows the convergence of a conservative state vector L_2 error with mesh refinement. Note that the ideal convergence is indicated by dash-dot lines with rates labeled. Table 4 and Table 5 tabulate the L_2 error with convergence rate. Figure 8 and Figure 7 draw a comparison of errors and convergence rates between different numbers of revolutions of the vortex transport. transport. Note that the convergence rates for 1-revolution results are labeled. Figure 9 shows the same error versus work units.

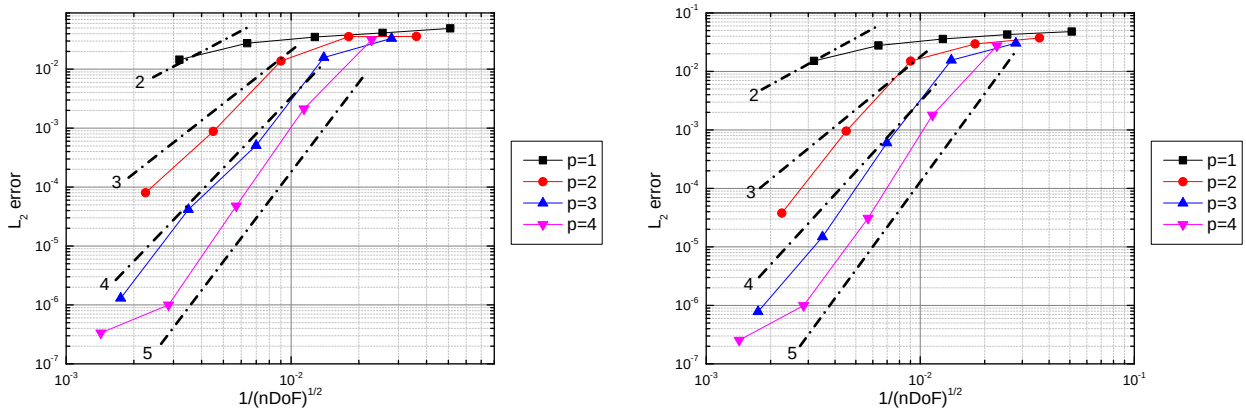

Unperturbed meshes

Perturbed meshes

Figure 2: Slow vortex: L_2 error convergence with mesh h refinement

nelem	$p=1$	$p=2$	$p=3$	$p=4$
128	4.9180e-02	3.6050e-02	3.3280e-02	3.1580e-02
rate	-	-	-	-
512	4.1220e-02	3.5710e-02	1.5800e-02	2.1300e-03
rate	0.25	0.01	1.07	3.89
2048	3.5120e-02	1.3750e-02	5.0673e-04	4.7800e-05
rate	0.23	1.38	4.96	5.48
8192	2.7630e-02	8.8162e-04	4.1600e-05	1.0000e-06
rate	0.35	3.96	3.61	5.58
32768	1.4480e-02	8.0000e-05	1.3000e-06	3.3600e-07
rate	0.93	3.46	5.00	1.57

Table 2: Slow vortex: L_2 error convergence with mesh h refinement for unperturbed meshes

nelem	$p=1$	$p=2$	$p=3$	$p=4$
128	4.8100e-02	3.7400e-02	3.0450e-02	2.7490e-02
rate	-	-	-	-
512	4.2650e-02	2.9480e-02	1.5550e-02	1.8000e-03
rate	0.17	0.34	0.97	3.93
2048	3.5810e-02	1.4990e-02	5.9847e-04	3.0996e-05
rate	0.25	0.98	4.70	5.86
8192	2.7790e-02	9.5451e-04	1.4810e-05	9.9568e-07
rate	0.37	3.97	5.34	4.96
32768	1.5130e-02	3.7790e-05	7.7881e-07	2.5419e-07
rate	0.88	4.66	4.25	1.97

Table 3: Slow vortex: L_2 error convergence with mesh h refinement for perturbed meshes

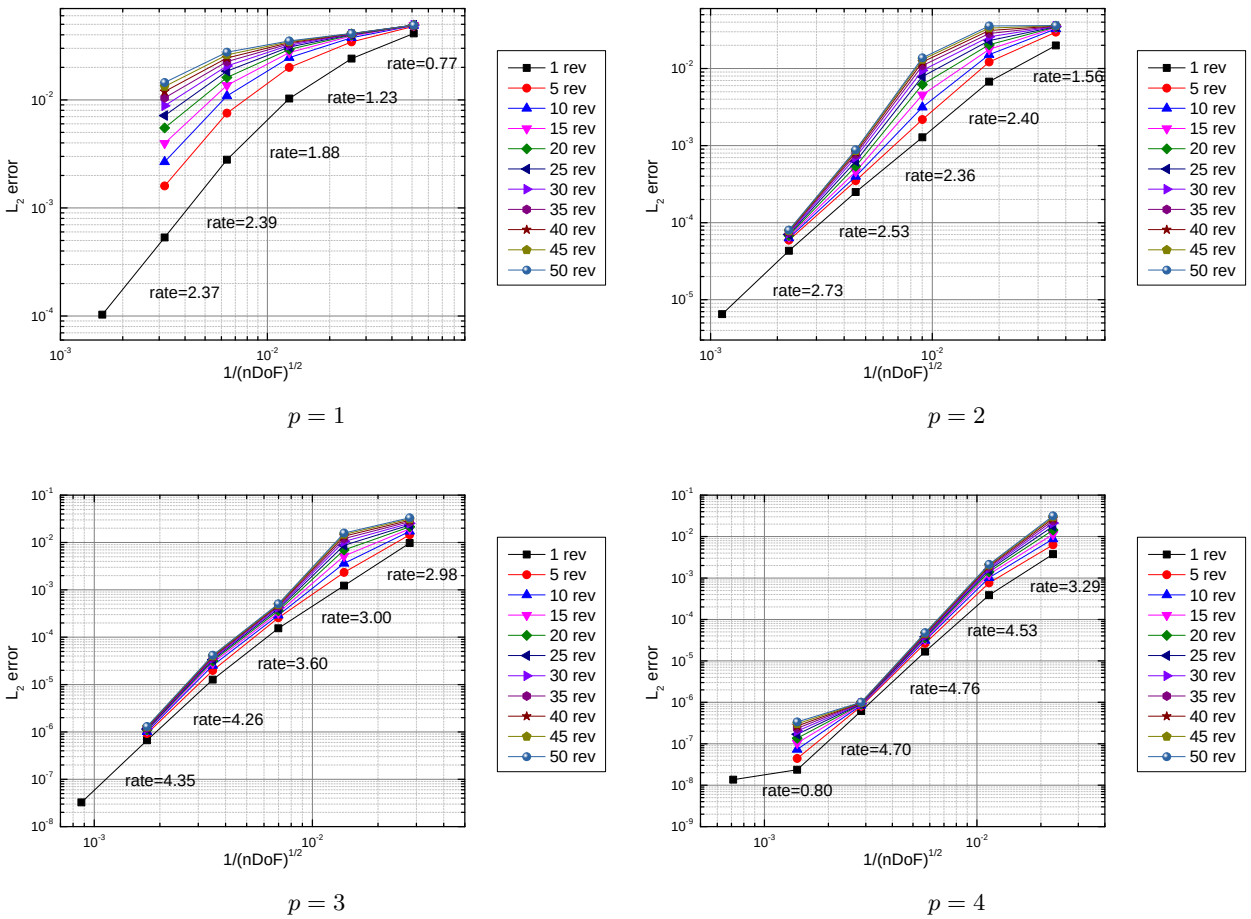

Figure 3: Slow vortex: L_2 error convergence with mesh h refinement for different revolutions using unperturbed meshes

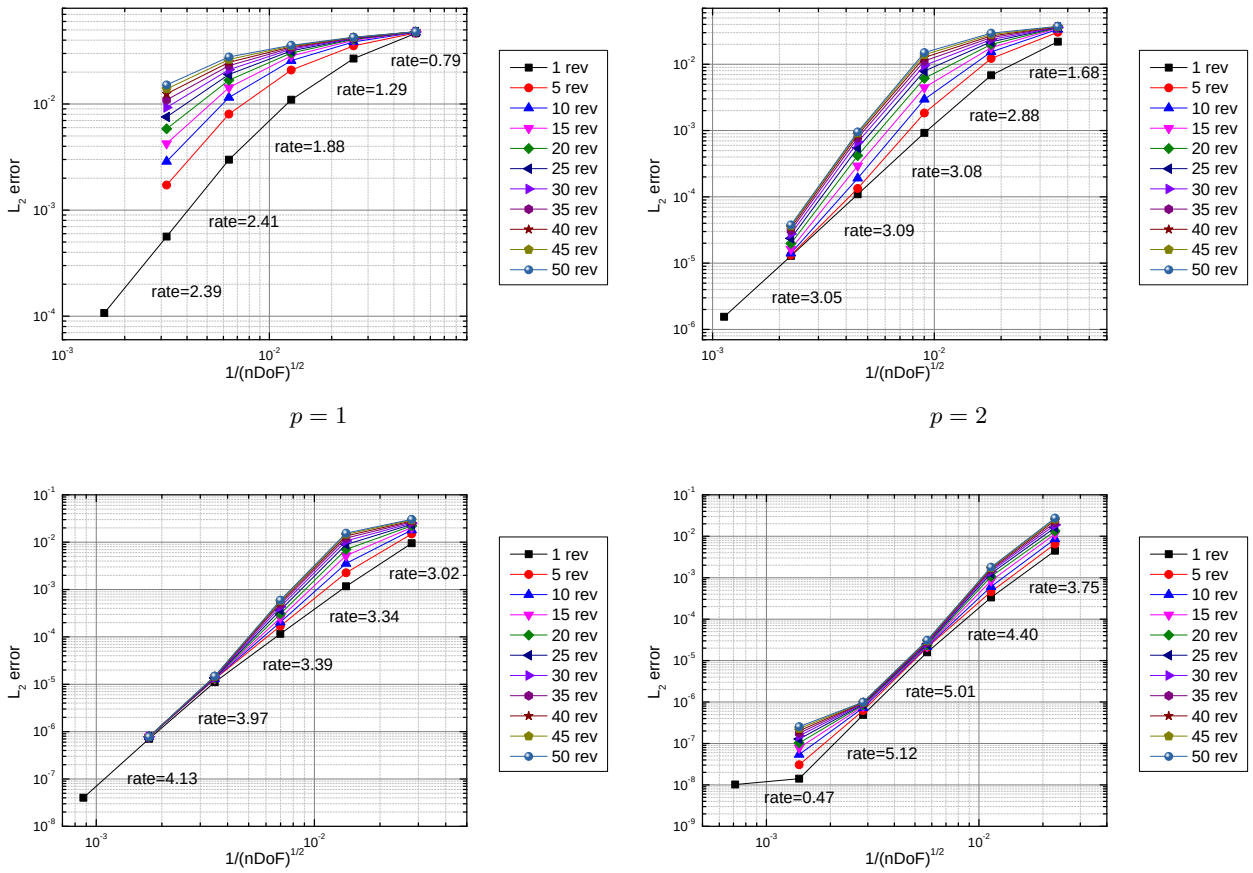

$p = 1$ $p = 2$

$p = 3$ $p = 4$

Figure 4: Slow vortex: L_2 error convergence with mesh h refinement for different revolutions using perturbed meshes

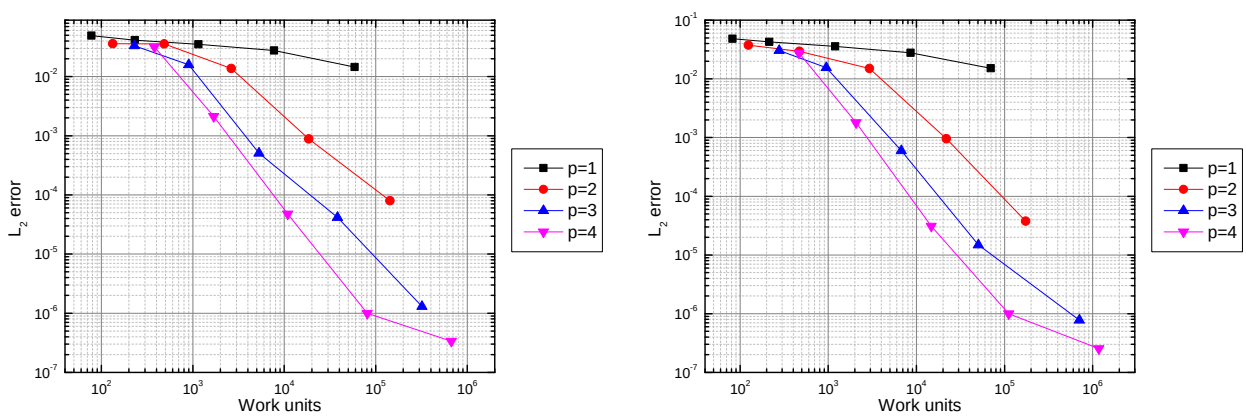

Unperturbed meshes Perturbed meshes

Figure 5: Slow vortex: L_2 error convergence with work units

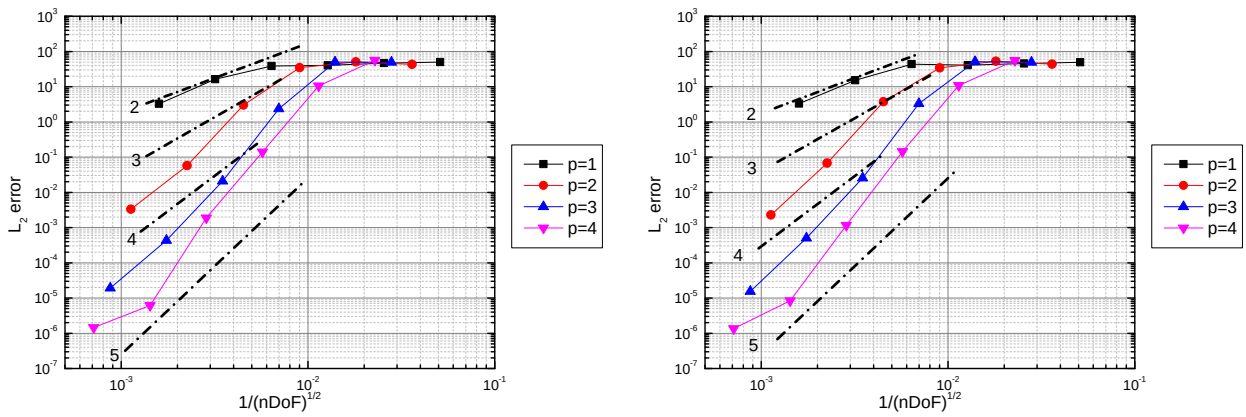

Unperturbed meshes

Perturbed meshes

Figure 6: Fast vortex: L_2 error convergence with mesh h refinement

nelem	$p=1$	$p=2$	$p=3$	$p=4$
128	4.9672e+01	4.2798e+01	4.9533e+01	5.5991e+01
rate	-	-	-	-
512	4.6378e+01	5.0752e+01	4.9606e+01	1.0603e+01
rate	0.10	-0.25	-0.00	2.40
2048	4.0346e+01	3.4414e+01	2.3594e+00	1.4111e-01
rate	0.20	0.56	4.39	6.23
8192	3.8452e+01	2.9956e+00	2.1010e-02	1.8900e-03
rate	0.07	3.52	6.81	6.22
32768	1.6364e+01	5.7300e-02	4.3537e-04	6.1109e-06
rate	1.23	5.71	5.59	8.27
131072	3.2417e+00	3.3100e-03	1.9045e-05	1.4406e-06
rate	2.34	4.11	4.51	2.08

Table 4: Fast vortex: L_2 error convergence with mesh h refinement for unperturbed meshes

nelem	$p=1$	$p=2$	$p=3$	$p=4$
128	4.9440e+01	4.3598e+01	4.9262e+01	5.5537e+01
rate	-	-	-	-
512	4.5561e+01	5.2355e+01	5.1469e+01	1.0823e+01
rate	0.12	-0.26	-0.06	2.36
2048	4.0546e+01	3.4233e+01	3.2824e+00	1.4411e-01
rate	0.17	0.61	3.97	6.23
8192	4.3493e+01	3.7359e+00	2.5700e-02	1.1600e-03
rate	-0.10	3.20	7.00	6.96
32768	1.5171e+01	6.7410e-02	5.0152e-04	8.4209e-06
rate	1.52	5.79	5.68	7.11
131072	3.2970e+00	2.2700e-03	1.5509e-05	1.3610e-06
rate	2.20	4.89	5.02	2.63

Table 5: Fast vortex: L_2 error convergence with mesh h refinement for perturbed meshes

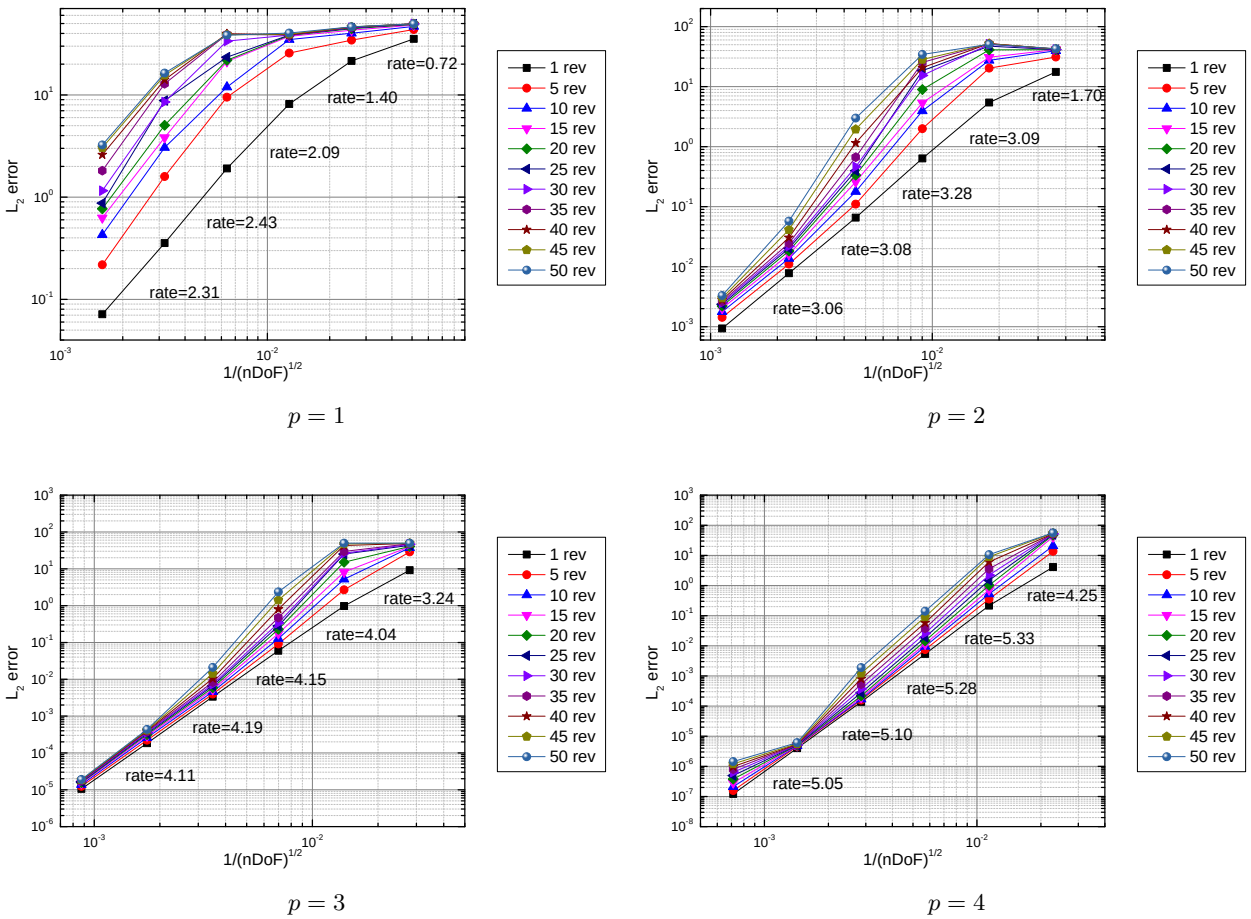

$p = 1$ $p = 2$

$p = 3$ $p = 4$

Figure 7: Fast vortex: L_2 error convergence with mesh h refinement for different revolutions using unperturbed meshes

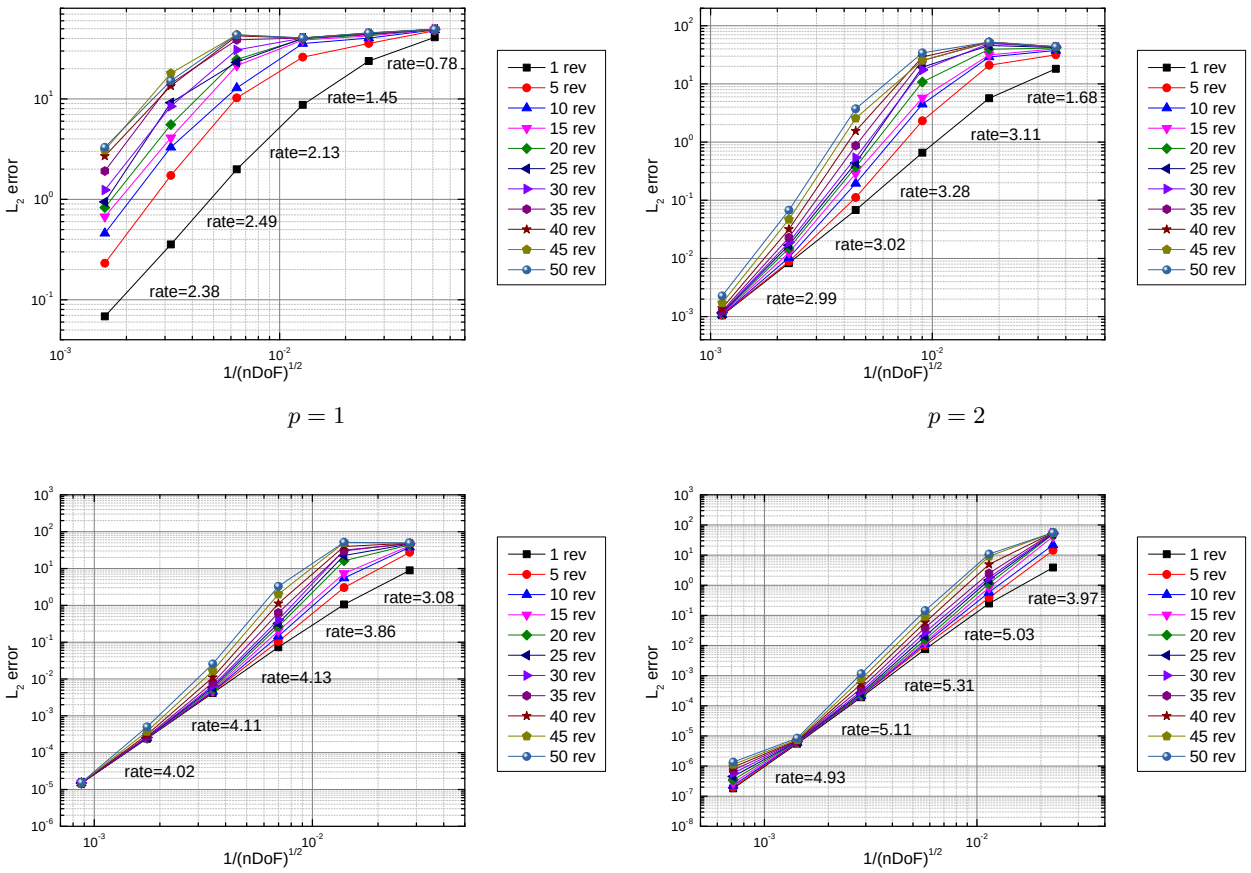

$p = 1$ $p = 2$

$p = 3$ $p = 4$

Figure 8: Fast vortex: L_2 error convergence with mesh h refinement for different revolutions using perturbed meshes

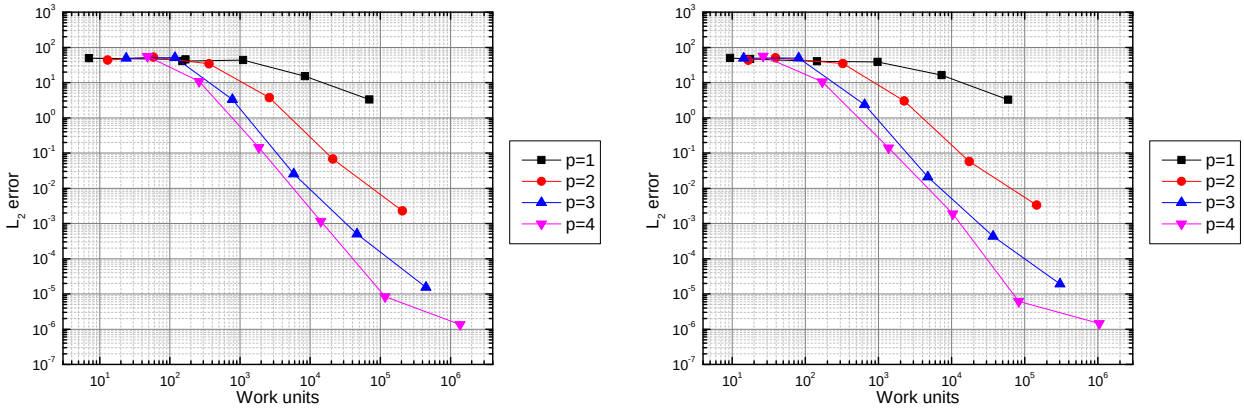

Unperturbed meshes Perturbed meshes

Figure 9: Fast vortex: L_2 error convergence with work units